High-Density ECR-Plasma Deposited Silicon Nitride Films for Applications in III/V-based Compound Semiconductor Devices

R. E. Sah[a], M. Mikulla[a], H. Baumann[b], F. Benkhelifa[a], R. Quay[a], and G. Weimann[a]

[a] Fraunhofer Institute for Applied Solid State Physics, Tullastrasse 72, D-79108 Freiburg, Germany,
E-mail:sah@iaf.fhg.de, Phone: ++49 761 51590
[b] Institut für Kernphysik, J. W. Goethe Universität, Max-von-Laue-Strasse 1, 60438 Frankfurt, Germany,
Phone: ++49 69 79847016

Keywords: High-density plasma, SiN film, ECR-PECVD, GaN HEMT, Passivation, Dielectric film

Abstract

We report on the ECR-plasma deposition and characterization of silicon nitride film exhibiting high breakdown field strength (>8 MV/cm) for applications in III/V-based compound semiconductor devices. The film deposited at 240°C contains around 13 at.% hydrogen. The hysteresis in mechanical stress, obtained from thermal cycling of the stress in film is negligible. The application of the film is being demonstrated in GaN-based HEMTs. The devices with gate length 0.3 µm and a periphery of 8x125 µm yielded cw output power density of 5.2 W/mm at 10 GHz and 35 V drain bias after passivation with the SiN film.

INTRODUCTION

Silicon nitride (SiN) thin films are widely used as dielectric and passivating layers in the fabrication of III/V-based electronic and optoelectronic devices [1]. Among other requirements for high-quality films, low hydrogen contents to avoid dopant passivation and blistering during annealing, low deposition temperature in order to minimize the interface defects, low intrinsic stress for eliminating the formation of crystal defects in the underlying layers as well as cracking of the films are of great importance. In addition, for application in high-power GaN HEMT devices, high breakdown field strength is necessary.

High-density plasma sources such as ECR plasma [2-3] and ICP [4-7] are increasingly used for the deposition of the films. The ECR-PECVD technique provides low ion energy bombardment and low plasma damage to devices [8-9]. In addition, the technique allows the deposition of SiN films at low deposition temperatures with a low amount of hydrogen [10]. It has also been reported that films deposited using ECR-PECVD technique have a superior water blocking ability than films deposited using conventional parallel-plate PECVD technique [11].

EXPERIMENTAL

For the deposition of the films a PlasmaTherm ECR-PECVD system (SLR 770) was used. The system was equipped with an ASTEX® AX4400 ECR plasma source and a load lock. The base pressure was $1.2x10^{-7}$ Torr. The films were deposited from SiH_4, N_2, and Ar as precursors. The mixture of Ar and N_2 was introduced in the ECR source, while undiluted SiH_4 was introduced in the deposition chamber through a gas dispersal ring located a few cm above the substrate.

The thickness and refractive index of the film were determined by measuring ellipsometric parameters Ψ and Δ with a SENTEC variable angle spectroscopic ellipsometer in the spectral range 1.55 – 4.13 eV and evaluating the measurements using Cauchy´s dispersion relation.

The determination of H content in the film is based on the nuclear reaction $^{15}N(^{1}H,\alpha,\gamma)^{12}C$ analysis [12]. The excitation function of this reaction shows a pronounced resonance in the cross-section at 6.385 MeV. By counting the 4.43 MeV γ-radiation for different energies of the probing ^{15}N ion beam, high resolution depth profiling is possible. The γ-rays from the nuclear reaction were measured with two 8´´x4´´ NaI detectors.

The concentrations of elements other than H were measured using n-RBS with 3.5 MeV ^{4}He projectiles at a scattering angle of 171° [13-15]. The backscattering cross-section for ^{14}N at 3.5 MeV is twice compared to the Rutherford cross section. The relative concentrations of Si and N in the films were determined by comparing experimental and simulated backscattering spectra using the computer program RUMP [16]. The film for n-RBS as well as for NRA measurements was deposited on a Si substrate.

The IR absorption spectra were measured using a Fourier Transform Bruker spectrometer Equinox 55. The AFM analysis was performed using Nanoscope III with an accuracy better than 2 % with NanoProbe silicon tips. The samples used for FTIR analysis ware bare GaAs test wafers deposited with SiN films, while those used for AFM analysis were patterned wafers. The electrical characterization of the film was performed on precisely patterned MIM capacitance test structures with 250 nm SiN film sandwiched between

two metal plates. The lower metal plate was evaporated on a 4´´-silicon wafer and was 350 nm thick. The upper metal plate was electroplated and was 7 μm thick.

The stress in the film was determined by measuring the changes in radius of curvature of 0.5 mm thick 2" in diameter s. i. GaAs wafer before and after deposition of the film using a FSM System (500TC) equipped with a dual laser optical lever. The thermal cycling was performed between room temperature and 400°C in N_2 atmosphere. The heating and cooling rates were 5°C per min.

RESULTS AND DISCUSSIONS

Fig. 1 illustrates the homogeneity in the thickness of the film on 4´´-GaAs wafer obtained from the ellipsometric measurements performed with 10 mm edge exclusion. As can be seen the variation in the thickness is better that ±5 %. The homogeneity in the refractive index of the film was ±0.5 % (Fig. 2).

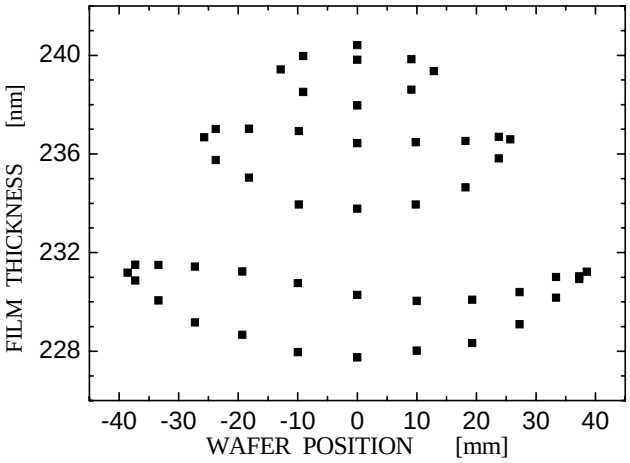

Fig. 1. Variation in thickness of the film on 4´´-GaAs wafer. 0 corresponds to center of the wafer.

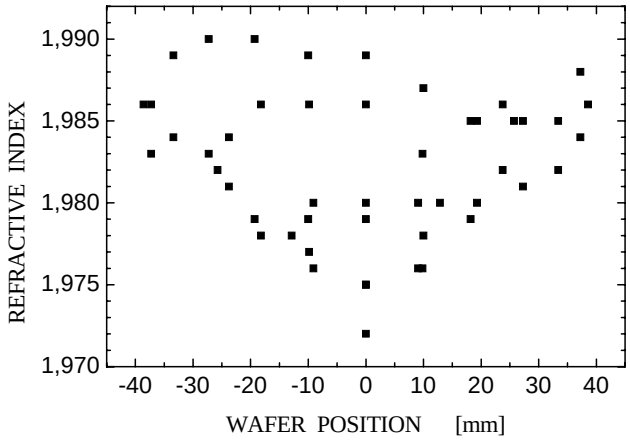

Fig. 2. Variation in refractive index of the film on 4´´-GaAs wafer. 0 corresponds to center of the wafer.

A typical RBS spectrum of the film is shown in Fig. 3. We observe Si and N signals as marked in the figure. We do not observe any O signal which indicates that the film is oxygen-free, i.e., not only the chemically bonded but also non-bonded O is absent in the film. Comparisons with simulated spectra indicated that the composition of this film is 43 at.% Si and 44 at.% N. NRA measurements revealed that the film contains around 13 at.% H. The hydrogen content for the sample was relatively constant with depth. Besides the concentrations of elements in the film the areal density in unit atoms/cm^2 was also obtained from the simulation. The areal density, concentrations of all elements and geometrical thickness of the film lead to the determination of density of the film. The density of the films thus determined from the results of RBS and NRA measurements was around 2.5 g/cm^3.

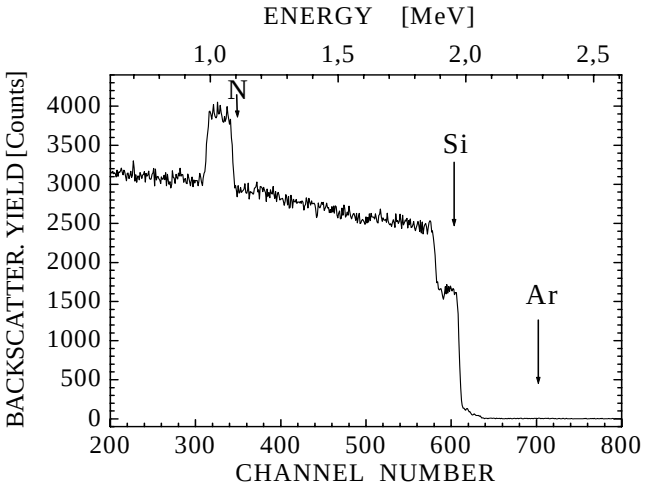

Fig. 3. RBS spectrum of SiN film deposited on Si substrate at 240°C.

The infrared (600-3600 cm^{-1}) absorption spectrum from the film is illustrated in Fig. 4. The spectrum shows well-resolved absorption peaks at 3300, 2150, 1150 and 885 cm^{-1}

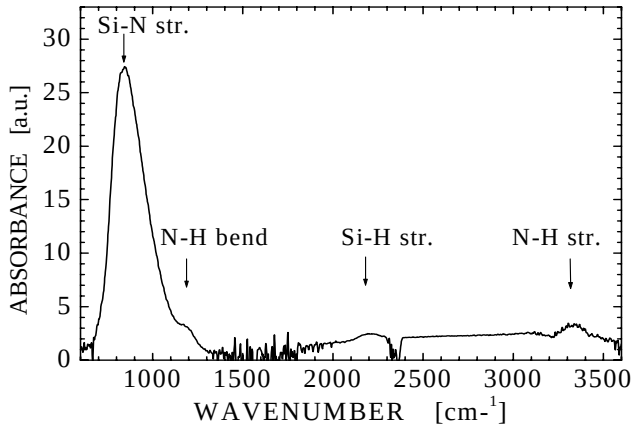

Fig. 4. Infrared spectrum from SiN film deposited on s.i. GaAs wafer.

attributed to N-H, Si-H and SiN stretching bonds, respectively. The shoulder at 1150 cm^{-1} is attributed to N-H bending bond. No oxygen containing bond due to impurity has been observed in the spectrum, although the measurements were performed a few weeks after the deposition. This indicates that the film does not oxidize in atmosphere.

Fig. 5 illustrates the change in stress in the film with thermal cycling between room temperature and 400°C. As can be seen, at room temperature the stress in the film is tensile 165 MPa, which increases linearly with temperature to 260 MPa at 400°C. Upon subsequent cooling from 400°C to room temperature, the stress change follows almost the same path as that of heating, thus exhibiting negligible hysteresis. The linear and reversible dependence of stress on temperature indicates that thermally induced expansion of the film and of the substrate are elastic in the temperature range measured and also the difference between both expansions is constant with temperature. From this it can be inferred that almost all hydrogen atoms in the film are chemically bonded so that there is nearly no desorption of H from the film.

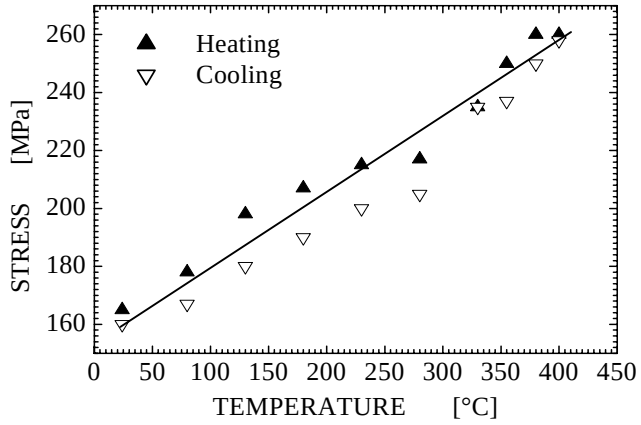

Fig. 5. Stress change in SiN film during first thermal cycling.

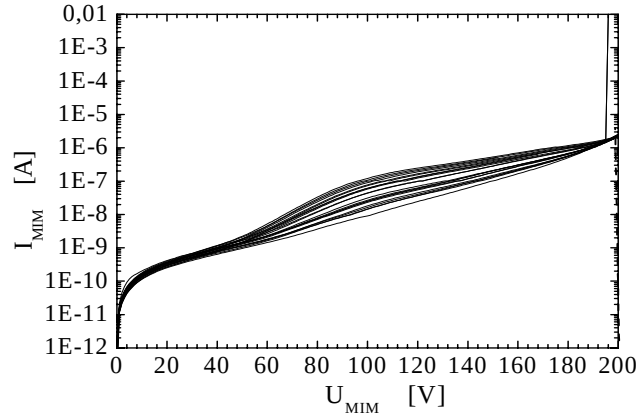

Fig. 6. I-V characteristics of 250x500 μm^2 MIM-capacitors with 250 nm thick SiN film as insulator deposited at 240°C.

The dc current-voltage characteristics of 250x500 μm^2 MIM capacitors with one of our SiN films developed for passivating GaN-based HEMT devices are presented in Fig. 6. The measurements were performed up to 200 V, the limitation being given by our instrumentation. The electric field strength corresponding to 200 V is 8 MV/cm. As is shown, most of the capacitors did not fail up to 200 V. The corresponding leakage current is $2x10^{-6}$ A. The capacitances and resistances of 200x500 μm^2 MIM are around 22 nF/cm^2 and 10^{12} ohm, respectively. Fig. 7 shows the capacitance density distribution for 200x500 μm^2 capacitors in the sample of Fig. 6. The sample contained capacitors of different geometrical dimensions. The yield of 200x500 μm^2 capacitors on the 4´´-Si wafer was 99 %, while that of 2x2 mm^2 capacitors on the same wafer was 51 %.

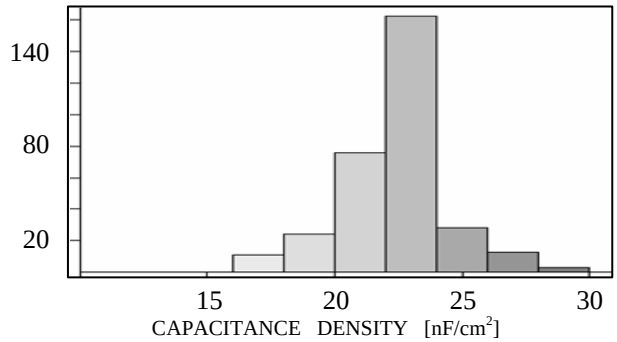

Fig. 7. Capacitance density distribution of a 4”-wafer.

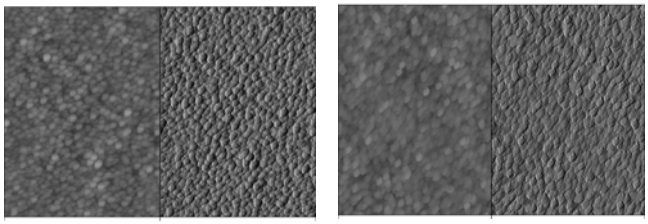

8(a), RMS=2.8 nm 8(b), RMS=2.8 nm

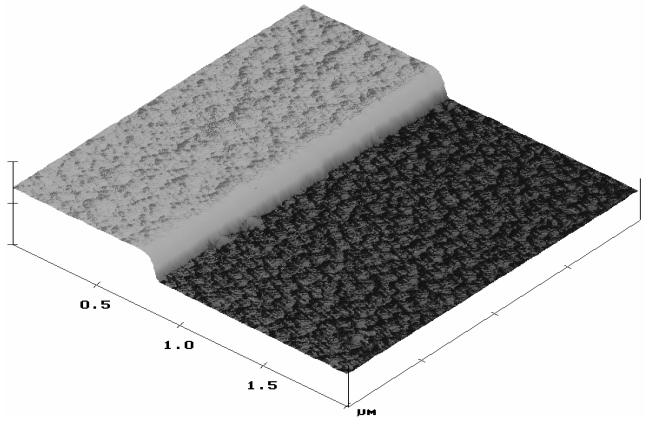

8(c)

Fig. 8. AFM images of (a) Metal 1 deposited on a Si substrate, (b) SiN film deposited on Metal 1, (c) Step coverage of Metal 1.

The RMS surface roughness obtained from AFM analysis (Fig. 8) does not change after the deposition of SiN film (Fig. 8a, and 8b). Furthermore, the SiN film is quite conformal and has excellent step coverage over the rough (RMS=46 nm) Metal 1 surface (Fig. 8c).

Fig. 9 shows the results of on-wafer microwave power measurements obtained after passivation of GaN-based HEMTs on 2´´-SiC wafer with the SiN film described in Fig. 5. The measurements were performed on the devices with gate lengths of 0.3 µm. The periphery of the device was 8x125 µm. The devices measured under cw at 10 GHz yielded a maximum output power density of 5.2 W/mm at 35 V drain bias, with a linear gain of 11 dB, and a maximum PAE of 31 % as shown in Fig. 9. The device yield was 80 % with an average maximum power density of 5 W/mm.

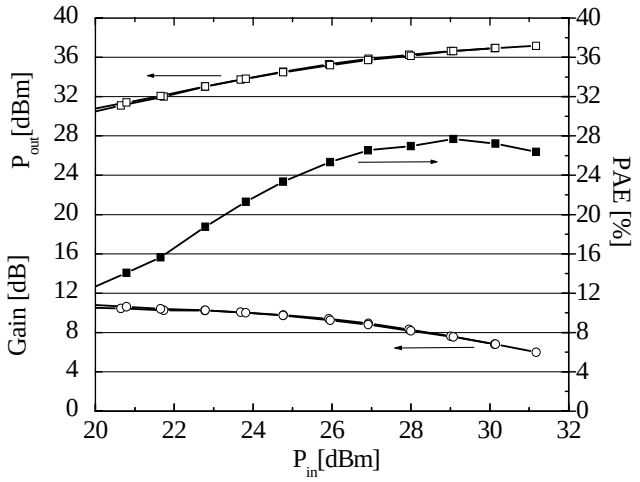

Fig. 9. Output power, PAE and gain of GaN-HEMT devices.

CONCLUSIONS

Using ECR-PECVD technique we have developed high-quality SiN films from a mixture of SiH_4, N_2, and Ar as precursors at a relatively low deposition temperature (240°C) containing a low amount of hydrogen. The films are quite conformal and has excellent step coverage over the rough metal. They exhibit a negligible hysteresis in mechanical stress and high breakdown electric field strength. The film has been successfully used in the passivation of GaN-based HEMTs. The devices with gate length 0.3 µm and a periphery of 8x125 µm yielded cw output power density of 5.2 W/mm at 10 GHz after passivation with the SiN.

ACKNOWLEDGEMENTS

The authors would like to thank G. Kaufel, N. Gruen, J. Ruester for electrical measurements and D. Luick for infrared spectroscopic measurements.

REFERENCES

[1] F. H. P. M. Habraken and A. E. T. Kuiper, Mater. Sci. Eng., **R12**, 123 (1994).
[2] S. Matsuo and K. Kikuchi, Jpn. J. Appl. Phys., Part 2, **66**, L210 (1988).
[3] J. C. Barbour, H. J. Stein, O. A. Popov, M. Yoder, and C. A. Outten, J. Vac. Sci. Technol. A, **9**, 480 (1991).
[4] Y. C. Chou et al.., *Novel Nitride passivation om 0.15 µm Pseudomorphic GaAs HEMTs Using High-Density Inductively Coupled Plasma CVD (HD-ICP-CVD), 2002* GaAs MANTECH Technical Digest, pp. 91-94, 2002.
[5] Y. C. Chou et al.., *On the Development of High Density Nitrides for MMICs,, 2003* GaAs MANTECH Technical Digest, pp. 61-64, May 2003.
[6] J. H. Zhou, C. Sinn, C. Hodson, R. Kinsey, C. D. W. Wilkinson, Proc. 16th International Symposium on Plasma Chemistry, Taormina, Italy, June 22-27, 2003.
[7] K. Elgaid, et al.., *Low Temperature High Density Highly Uniform Si_3N_4 Technology for Passive and Active Devices in MMMIC Applications*, 2003 GaAs MANTECH Technical Digest, pp. 311-313, May 2004.
[8] R. E. Sah et al., in *State-of-the–Art Program on Compound Semiconductors XXVI*, D. N. Buckley et al., eds., PV **97-1**, p. 178, The Electrochemical,Society Proceedings Series, Pennington, NJ (1997).
[9] Q. Wang, E. S. Yang, P. W. Li, Z. Lu, R. M. Osgood, Jr., and W. I. Wang, *IEEE Electron Device Lett*., ED-**13,** 82 (1992).
[10] R. E. Sah and H. Baumann, in *State-of-the–Art Program on Compound Semiconductors XXIV*, F. Ren et al., eds., PV **96-2**, p. 214, The Electrochemical,Society Proceedings Series, Pennington, NJ (1996).
[11] S. Okuda, Y. Shioya, and H. Kashimada, J. Electrochem. Soc. **145**, 1338 (1998).
[12] W. A. Lanford, Nuclear Reactions for Hydrogen Analysis, in *Handbook of Modern Ion Beam Materials Analysis*, J. R. Tesmer et al., eds., p. 193, Materials Research Society, Pittsburgh, PA (1995).
[13] J. A. Leavitt and L. C. McIntyre, Jr., in *Handbook of Modern Ion Beam Materials Analysis*, J. R. Tesmer, M. Nastasi, eds., p. 39, Mater. Res. Soc., Pittsburgh, PA (1995).
[14] D. F. Herring, Phys. Rev., **112**, 1217 (1958).
[15] L. R. Doolittle, Nucl. Instr. Methods **B, 15**, 227 (1986).
[16] R. L. Pfeffer, G. J. Geradi, R. A. Lux, K. A. Jones, E. H. Poindexter, W. H. Chang, and R. A. B. Devine, Mat. Res. Soc. Proc., **165**, 227 (1990).

ACRONYMS

AFM: Atomic Force Microscopy
cw: continuous wave
dc: direct current
ECR: Electron Cyclotron Resonance
FTIR: Fourier Transform Infrared
GaN: Gallium Nitride
HEMT: High Electron Mobility Transistor
ICP: Inductively Coupled Plasma
MIM: Metal Insulator Metal
n-RBS: Non-Rutherford Backscattering Spectroscopy
NRA: Nuclear Reaction Analysis
PAE: Power-Added Efficiency
PECVD: Plasma-Enhanced Chemical Vapor Deposition
RMS: Root Mean Square